Neurobiology of Stress 13 (2020) 100280

Contents lists available at ScienceDirect

Neurobiology of Stress

journal homepage: www.elsevier.com/locate/ynstr

# LSD1 is an environmental stress-sensitive negative modulator of the glutamatergic synapse

A. Longaretti [a], C. Forastieri [a], E. Toffolo [a], L. Caffino [b], A. Locarno [c], I. Misevičiūtė [c], E. Marchesi [d], M. Battistin [a], L. Ponzoni [e], L. Madaschi [f], C. Cambria [a], M.P. Bonasoni [g], M. Sala [e], D. Perrone [d], F. Fumagalli [b], S. Bassani [e], F. Antonucci [a], R. Tonini [c], M. Francolini [a], E. Battaglioli [a,1], F. Rusconi [a,*,1]

[a] Dept. of Medical Biotechnology and Translational Medicine, Università Degli Studi di Milano, Via F.lli Cervi, 93, Segrate (MI), Italy
[b] Dept. of Pharmacological and Biomolecular Sciences, Università Degli Studi di Milano, Via Balzaretti, 9, Milano, Italy
[c] Neuromodulation of Cortical and Subcortical Circuits Laboratory, Istituto Italiano di Tecnologia, Via Morengo, 30, Genova, 16163, Italy
[d] Dept. of Chemical and Pharmaceutical Sciences, Università di Ferrara, Via Borsari, 46, Ferrara, Italy
[e] Institute of Neuroscience, Consiglio Nazionale Delle Ricerche (CNR), Via Vanvitelli, 32, Milan, Italy
[f] UNITECH NO LIMITS, Università Degli Studi di Milano, Via Celoria, 26, Milan, Italy
[g] ASMN Santa Maria Nuova Via Risorgimento, 80 Reggio Emilia, Italy

ARTICLE INFO

*Keywords:*
LSD1/KDM1A
Psychiatric disorders
Environmental stress
REST/NRSF
Neuroplasticity
Alternative splicing
Epigenetics
Glutamatergic synapse
Aging

ABSTRACT

Along with neuronal mechanisms devoted to memory consolidation –including long term potentiation of synaptic strength as prominent electrophysiological correlate, and inherent dendritic spines stabilization as structural counterpart– negative control of memory formation and synaptic plasticity has been described at the molecular and behavioral level. Within this work, we report a role for the epigenetic corepressor Lysine Specific Demethylase 1 (LSD1) as a negative neuroplastic factor whose stress-enhanced activity may participate in coping with adverse experiences. Constitutively increasing LSD1 activity via knocking out its dominant negative splicing isoform neuroLSD1 (neuroLSD1$^{KO}$ mice), we observed extensive structural, functional and behavioral signs of excitatory decay, including disrupted memory consolidation. A similar LSD1 increase, obtained with acute antisense oligonucleotide-mediated neuroLSD1 splicing knock down in primary neuronal cultures, dampens spontaneous glutamatergic transmission, reducing mEPSCs. Remarkably, LSD1 physiological increase occurs in response to psychosocial stress-induced glutamatergic signaling. Since this mechanism entails neuroLSD1 splicing downregulation, we conclude that LSD1/neuroLSD1 ratio modulation in the hippocampus is instrumental to a negative homeostatic feedback, restraining glutamatergic neuroplasticity in response to glutamate. The active process of forgetting provides memories with salience. With our work, we propose that softening memory traces of adversities could further represent a stress-coping process in which LSD1/neuroLSD1 ratio modulation may help preserving healthy emotional references.

## 1. Introduction

Since decades researchers work to discover how the environment influences biological processes, in particular those active in the brain. This momentous effort stems from an empirical certainty: environmental stress (and its implicit toxicity) represents a driving factor for the onset of mental illnesses. Acute traumatic events must be learned and memorized within an adaptive process that improves survival. Indeed context-driven recall of a threatful memory helps raising vigilance as well as avoidance-instrumental behaviors (Popoli et al., 2012; Sanacora et al., 2012). However, stressful events couple to learning responses also an important affective counterpart, promoting for instance neuroendocrine enhancement of glutamatergic function (Popoli et al., 2012; Yang et al., 2005). Adverse experiences indeed trigger intense glutamate release at emotionally-relevant amygdalar and hippocampal synapses, in such a way that environmental stress is the only external insult capable of facilitating glutamate spill-over at dendritic spines (Yang

* Corresponding author.
*E-mail address:* francesco.rusconi@unimi.it (F. Rusconi).
[1] These authors equally contributed to the work.

https://doi.org/10.1016/j.ynstr.2020.100280
Received 15 August 2020; Received in revised form 19 November 2020; Accepted 22 November 2020
Available online 27 November 2020

**Abbreviations**

| | |
|---|---|
| ABHD6 | α/β Hydrolase domain containing 6 |
| AMPAR | α-Amino-3-hydroxy-5-Methyl-4-isoxazolePropionic Acid Receptor |
| AON | Antisense Oligonucleotide |
| 2-AG | 2-Arachidonyl Glycerol |
| ASDS | Acute Social Defeat Stress |
| CB1R | Cannabinoid 1 Receptor |
| CoREST | Corepressor of REST |
| eCB | Endocannabinoids |
| ECS | Endocannabinoid System |
| EGR1 | Early Growth Response 1 |
| fEPSPs | field Excitatory Post Synaptic Potentials |
| HDAC2 | Histone Deacetylase |
| H3K4 | Histone H3 Lysine 4 |
| HSR | Homeostatic Stress Response |
| IEGs | Immediate Early Genes |
| LSD1 | Lysine Specific Demethylase 1 |
| LTD | Long Term Depression |
| LTP | Long Term Potentiation |
| MAGL | Monoacylglycerol lipase |
| mEPSC | minis Excitatory Post Synaptic Currents |
| mIPSC | minis Inhibitory Post Synaptic Currents |
| NMDAR | N-Methyl-D-Aspartate Receptor |
| 2′-OMe | 2′-*O*-methyl |
| OTF | Oligothiophene fluorophore |
| PS | Phosphorothioate |
| REST | RE-1 Silencer Transcription Factor |
| RPL13 | Ribosomal Protein L13 |
| RPSA | Ribosomal Protein SA |
| TEM | Transmission Electron Microscopy |
| SBS-SEM | Serial Block Face Scanning Electron Microscopy |
| SCRA | scramble |
| SPF | Specific Pathogen Free |

et al., 2005), potentially coupled to the risk of excitotoxic-related circuitry issues (Duman, 2009; Kang et al., 2012; Diamond et al., 2007). Within a successful stress response, potential glutamate-induced toxicity –and related behavioral negative effects– is prevented by efficient molecular homeostatic processes, concomitantly engaged by stress (Rodríguez-Muñoz et al., 2016; Cadle and Zoladz, 2015). Remarkably, a further aim of these homeostatic neuronal defenses is to regulate learning and memory of the adverse experience (Rusconi and Battaglioli, 2018).

Examples of *homeostatic stress response* (HSR) have been described, being the endocannabinoid system (ECS) the best established so far. ECS indeed represents a fast-acting negative synaptic feedback, gradually downsizing stress-elicited neurotransmitter release instrumentally to stress response termination (Morena et al., 2016; Lutz et al., 2015; Rusconi, 2020). ECS (in particular through 2-arachidonyl glycerol, 2-AG), also exerts a negative modulation of memory formation coupled to glutamate release inhibition, whose adaptive means should be further investigated in the frame of described 2-AG anxiolytic activity (Iannotti et al., 2016; Prini et al., 2018; Guggenhuber et al., 2015; Bluett et al., 2017; Patel et al., 2016; Shonesy et al., 2014). Not only glutamate release, but also its nuclear transduction leading to activation of neuroplasticity-relevant transcriptional programs is homeostatically targeted by epigenetic mechanisms (Rusconi and Battaglioli, 2018; Rusconi et al., 2020). At the nuclear level for instance, stress-induced DNA methylation of Immediate Early Genes (IEGs) promoters attenuates c-fos and egr1 transactivation in the hippocampus, scaling back behavioral stress responses (Saunderson et al., 2016) in the frame of a normal adaptive self-regulation (Carver and Scheier, 2000). Egr1 promoter methylation, in particular, increases in response to both forced swim stress (Saunderson et al., 2016) and fear conditioning (Gupta et al., 2010), seemingly representing a key molecular mechanism that softens learning and memory consolidation of adversities to a lesser (adaptive) extent. IEGs transcription is similarly buffered in response to stress by another transcriptional homeostatic system: the dual splicing rheostat Lysine Specific Demethylase 1 (LSD1)/neuroLSD1. Corepressive activity of LSD1, a flavin-dependent H3K4 histone demethylase, is counteracted in neurons by brain-restricted neuroLSD1, a dominant negative LSD1 alternative splicing isoform including microexon E8a (Wang et al., 2015; Toffolo et al., 2014). In particular, LSD1/neuroLSD1 relative ratio sets the specific strength of IEGs transcriptional responsivity through the modulation of histone H3K4 methylation, and H3K9/14 acetylation in the mouse hippocampus (Wang et al., 2015; Rusconi et al., 2016, 2017). In wild type mice, neuroLSD1 splicing-operated decrease (and concomitant LSD1 upregulation) is physiologically promoted by stress and similarly to stress-evoked DNA methylation (Saunderson et al., 2016), it attenuates in the hippocampus stress-induced IEGs transcription helping limiting anxiety arousal at the behavioral level (Rusconi et al., 2016, 2017).

If we consider that one of the leading aspects of Post-Traumatic Stress Disorder (PTSD) actually relies on excessive consolidation of traumatic memories, enriched with a plethora of vivid sensory details that tremendously reduce the threshold of associative recall probability, a provocative albeit realistic hypothesis can be ventured into: some of the effects of stress traditionally recognized as toxic and related to stress-induced amnesia –including disruption of Long Term Potentiation (LTP), increased Long Term Depression (LTD) probability in the hippocampus of previously stressed rodents, and memory loss (Diamond et al., 2007; Wong et al., 2007)– could instead be interpreted as adaptive, temporary responses whose efficacy is maximal in acute stress response (Diamond et al., 2007; Cadle and Zoladz, 2015).

Considering the crucial function of IEGs transcription in memory formation and neuroplasticity, in this work we further investigated the role of neuroLSD1 downregulation (and complementary LSD1 increase) in response to psychosocial stress as a temporary adaptive mechanism to cope with acute stress opposing to memory consolidation. Notably, LSD1 implications as suppressor of neuroplasticity can also be foreseen as one of its tighter cofactors, Histone Deacetylase 2 (HDAC2), has been extensively addressed as negative regulator of memory formation and synaptic plasticity (Guan et al., 2009). Recently we demonstrated that in response to stress, LSD1 directly enhances homeostatic activity of the ECS (Longaretti et al., 2020) further strengthening its implications in stress coping. In this work, exploring the nature of environmental LSD1 regulation, we discovered that LSD1/neuroLSD1 ratio is itself controlled by glutamatergic transmission. Hence LSD1 and neuroLSD1 are involved in a prototypic negative feedback mechanism in which NMDAR activation elicits neuroLSD1 downregulation that, in turn, limits post-synaptic glutamate responses. To better refine its functional neuronal domain, we provide additional evidence of molecular, structural and electrophysiological read outs of *LSD1* homeostatic feedback activity in the hippocampus, pushing forward its putative, adaptive contribution to forgetting negative experiences.

## 2. Material and methods

*Experimental animals.* Animals were housed in a SPF animal facility. 3-Month-old male CD1 (RRID:IMSR_CRL:22) and nine to ten-week-old male C57BL/6N (RRID:IMSR_CRL:027), neuroLSD1 heterozygous and neuroLSD1 knock out (neuroLSD1$^{KO}$) littermates, were housed at

controlled temperature (20–22 °C) with free access to food and water in a 12-hr light/dark cycle (lights on at 7:00 a.m.). In this study, we used a total number of 232 mice including 8 CD1 (ex-breeder) 224 C57BL/6N (wild type and neuroLSD1$^{HET}$ and knock outs). Among C57BL/6N we used 54 naïve mice and 178 manipulated mice. All experimental procedures involving animals followed the Italian Council on Animal Care guidelines (decree no. 26, March 2014) and European regulations (2010/63/UE) Italian Ministry of Health approval 275/2015 and 322/2018. Every effort was made to accomplish to the "3R" regulations. Anesthesia was performed with isofluorane.

*Total RNA extraction, qRT-PCR analysis, and rqfRT-PCR.* Total RNA isolation from hippocampal extract, qRT-PCR and rqfRT-PCR analyses were performed as in (Rusconi et al., 2016). Target gene expression was normalized on Ribosomal Protein SA (RPSA) of Ribosomal Protein L13 (RPS13). RPL13 expression stability along with aging was analyzed using Microsoft excel-based tool BestKeeper (Pfaffl et al., 2004). RNA integrity numbers (RIN) was assessed using RNA 6000 Nano Chips on Agilent 2100 bioanalyzer. In case of RNA from human post-mortem specimens, only samples with RIN between 4.6 and 7.5 were further analyzed (Le François et al., 2018).

*Golgi Staining.* Golgi Cox impregnation was performed with FD Rapid Golgi staining kit (FD NeuroTechnology) following manufacturers' instructions on PBS-perfused mice. Brains were coronally sliced (400 μm thickness) using a vibratome (Leica VT1000S). Images were acquired with a 63x/1.4 oil objective (Leika DM LB2) microscope and analyzed with Stereo Investigator software (MBF Bioscience).

*Transmission Electron microscopy (TEM).* Mice were transcardially perfused with 2.5% glutaraldehyde, 2% paraformaldehyde in 0.15 M sodium cacodylate buffer (pH 7.4). Dissected brains were processed described elsewhere (Murru et al., 2017). For quantitative analyses, TEM images were acquired at a final magnification of 25,000–46,000x with a Philips CM10 TEM using a Morada CDD camera (Olympus, Munster - Germany). Quantitative measurements were performed with ImageJ 1.51 as described (Murru et al., 2017). Evaluation of synapse density from 2D TEM images was performed according to the size-frequency stereological method as described in (Folci et al., 2016).

*Serial block face scanning electron microscopy (SBF-SEM).* Brain coronal sections (100 μm thickness) where obtained with a vibratome (Leica VT1000S). Hippocampi were manually dissected from these sections and processed for SBF-SEM, as described in (Vezzoli et al., 2020). SBF data-sets were collected using an APREO Volume Scope SEM (Thermo-fisher Scientific) operating at an accelerating voltage of 1.8 kV with high vacuum. Data were collected with a pixel size of 10 nm along the x, y-axis and 40 nm along the z-axis. The resulting datasets were assembled into volume files aligned using ImageJ, and then manually segmented into 3D models. Three-dimensional structures in image stacks containing hundreds or thousands of 2D orthoslices are traced individually in each plane and surface rendered.

*Preparation of Protein Extracts and Western Blot Analyses*. Hippocampal proteins of whole homogenate and post-synaptic density fraction were analyzed as previously described (Caffino et al., 2018) with minor modifications. Primary antibodies conditions are indicated in supplementary material and methods. Results were standardized using β-actin. Gels were run 3 times each and results represent the average from 3 different western blots (Colombo et al., 2017).

*Cell culture and transfection.* Rat primary hippocampal neurons were prepared from Sprague Dawley rat embryos at E18 (Romorini et al., 2004). Neurons were cultured and transfected with pEGFP plus either HA-pCGN vector (control) or HA-neuroLSD1 (neuroLSD1) as in (Zibetti et al., 2010). Images of pyramidal neurons were acquired with a Zeiss LSM510 confocal microscope (Carl Zeiss, Italy; gift from F. Monzino) by using a 63x/1.4 oil objective.

*Pharmacological treatments*. DIV 14 rat primary neurons were treated with Bicuculline 40 μM (Sigma-Aldrich) for 30 min, washed out and harvested at 8 h. NMDA 50 μM (Sigma-Aldrich) was left 10 min in neuron medium, washed out and analyses were performed 30 min, 2, 3, 7 and 8 h. APV 100 mM and MK-801 10 μM (Sigma-Aldrich) were added to the culture media immediately before NMDA and left for the entire length of the treatment. In vivo, 30 min prior the stress paradigm, experimental animals were intraperitoneally injected either with sterile NaCl 0.9% solution (VEH) or with MK-801 0.3 mg/kg.

*AON synthesis.* AONs used in this study are listed in supplementary materials and methods section. All AONs contain 2′-O-methyl modified RNA and full-length phosphorothioate backbone. Oligonucleotide syntheses and purifications were carried out at Università degli Studi di Ferrara (Ferrara, Italy), using Äkta instruments and following a well-established protocol (Rimessi et al., 2009). Fluorophore-labeled oligonucleotides were synthesized by reacting the commercial succinimidyl derivative of oligothiophene fluorophore OTF (Mediteknology S.r.l, Italy) with the primary amine group of the ssH-linker, previously attached to the 5′-end AON-21-E8a and AON-21-SCRA. Several thiophene fluorophores have been reported for the selective labeling of intracellular proteins and the fluorescence behavior of several AON-oligothiophene conjugates has been explored in model studies (Capobianco et al., 2012). Nevertheless, to the best of our knowledge, this is the first study considering the use of oligothiophene fluorophore OTF as fluorescent marker of AONs in live cells. To support our choice, absorption and photoluminescence spectra of OTF were in agreement with the required experimental conditions, OTF also showed good fluorescent properties and stability to bleaching even under prolonged irradiation. Finally, but not less important, OTF was non-sterically hindered, nontoxic to the cells, chemically stable, easy to handle and cost-effective when compared to other widely known oligonucleotide labeling, thus enabling its use for large-scale applications. The purity of full-length desired products was evaluated by HRMS, 31P-NMR and RP-HPLC analyses.

*AON treatments.* For Minigene reporter assay (Hybrid Minigene Construct MG800Δpal was generated as previously described (Baralle and Baralle, 2005; Rusconi et al., 2014)), cells in 35 mm wells were cotransfected 24 h after seeding with 1,25 μg MG800Δpal per 4 μl transfectant mix and along with 10–25–50 nM –concentration referred to transfectant mix– AON-E8a-21 or AON-SCRA-21, using Lipofectamine 2000 (Thermo Fisher Scientific) as transfection reagent, and analyzed 48 h after. For primary neurons cultures, AON-E8a-21 or AON-SCRA-21 were administered directly to the culture media at the concentrations of 0,5–2,5 - 15–25 μM, at DIV13 for 36 h.

*Electrophysiological* in vitro *recordings.* DIV13 high density cultured hippocampal neurons were treated with 15 μM antisense oligonucleotide AON-E8a-21 or AON-SCRA-21. Electrophysiological experiments were performed 36 h later. Excitatory and inhibitory post synaptic currents in miniature (mEPSCs and mIPSCs) have been measured by patch-clamp recordings in the whole-cell voltage clamp modality using Axopatch 200B amplifier and pClamp-10 software (Axon Instruments) as in (Antonucci et al., 2012). Recorded traces have been analyzed using Clapfit-pClamp 10 software, after choosing an appropriate threshold. For further details consult the supplementary materials and methods section.

*Ex-vivo electrophysiological recordings.* Mice were anesthetized with isofluorane and decapitated, and their brains were transferred to ice-cold dissecting modified-artificial cerebrospinal fluid (aCSF). Coronal sections (350 μm thick for field recordings or 250 μm thick for patch-clamp recordings) were cut using a Vibratome 1000S (Leica, Wetzlar, Germany). Following 20 min of incubation at 32 °C, slices were kept at 22–24 °C. During experiments, slices were continuously superfused with aCSF at a rate of 2 ml/min at 28 °C. Extracellular recordings of field postsynaptic potentials (fPSP) were obtained in the CA1 stratum radiatum, using glass micropipettes filled with artificial Cerebral Spinal Fluid (aCSF). Stimuli (50–160 μA, 50 μs) to excite Shaffer collaterals were delivered through a bipolar twisted tungsten electrode placed ≈400 μm from the recording electrode. Long-Term Potentiation (LTP) was induced using the following theta burst stimulation protocol (TBS): 10 trains (4 pulses at 100 Hz) at 5 Hz, repeated twice with a 2-min interval.

Long-Term Depression (LTD) was induced using a Low-frequency stimulation protocol (LFS) consisting of 900 pulses at 0.5Hz. The magnitude of LTP or LTD was evaluated by comparing the fPSP normalized slopes from the last 5 min of baseline recordings with those 40–50 min after TBS or LFS. For patch-clamp experiments, whole-cell recordings were made under direct IR-DIC (infrared-differential interference contrast) visualization of neurons in the hippocampal CA1 stratum pyramidale region. Excitatory postsynaptic currents (EPSCs) were evoked in the presence of the $GABA_A$ receptor antagonist gabazine (10 μM) by stimulation of stratum radiatum by using a theta glass electrode (20 μsc–80 μsc, 0.02 mA–0.1 mA) connected to a constant-current isolation unit (Digitimer LTD, Model DS3) and acquired every 10 s. AMPA/NMDA ratio of each neuron was calculated as the ratio between AMPA EPSC peak amplitude (pA) of the subtracted current and the NMDA EPSC peak amplitude (pA). For further details consult the supplementary materials and methods section.

*Acute Social Defeat Stress.* CD1 aggressor mice were used to defeat 2-month-old C57BL/6N wild-type mice in a 7-h-long session of psychosocial stress as previously described (Rusconi et al., 2016; Italia et al., 2020). All controls were sham-handled to subtract the manipulation effect. For further details consult the supplementary materials and methods section 8.

*Novel Object Recognition Test.* Novel Object recognition test was conducted as previously described (Leonzino et al., 2019). The discrimination index was calculated as described elsewhere (Pitsikas et al., 2001). For further details consult the supplementary materials and methods section.

*Human hippocampal samples*. Postmortem hippocampal samples derived from aged individuals (≥80-year-old people) were obtained from MRC London Neurodegenerative Diseases Brain Bank and associated brain banks, The Netherlands Brain Bank and BrainNet Europe, for all the others we collected samples from a dedicated study. Experimental protocols were approved by University of Milan Ethic Committee (n.40–18) and Territorial Ethic Committee AUSLR, (n. 2019/0004645). We used RPL13 as housekeeping gene to normalize gene expression. RPL13 expression is stable during aging, as verified using the Microsoft Excel-based tool BestKeeper (Pfaffl et al., 2004).

*Statistical analyses.* Data are shown as mean ± SEM. For single comparisons, we performed unpaired Student's *t*-Test or Mann-Whitney Test; for multiple comparisons, we either used one- or two-way ANOVA variance analyses associated to Tukey's post hoc test, only in case of statistical significance of the ANOVA test. To this aim we used GraphPad PRISM 8.0 software (RRID:SCR_002798). Verification of normal data distribution was performed for all experimental datasets taking advantage of GraphPad PRISM 8.0 software, applying the Shapiro–Wilk test. To retrieve outliers, we took advantage of GraphPad PRISM 8.0 software, applying ROUT method. We employed the number of experimental animals predicted by statistical sample size determination using the appropriate parameters (Power 0.8, α 0.05, β 0.2), within two independent study groups whose primary (continuous) endpoint is an average.

## 3. Results

### 3.1. Structural analyses unravel neuroplastic impoverishment in the hippocampus of neuroLSD1$^{KO}$ mice

Behavioral characterization of neuroLSD1$^{KO}$ mice, showing reduced vulnerability to neuronal hyperexcitability (Rusconi et al., 2014) and decreased anxiety profile (Rusconi et al., 2016), suggested diminished E/I ratio. To define whether the central excitatory synapse was influenced by neuroLSD1 modulation in the mouse brain, we performed electron microscopy (EM) studies focused on hippocampal CA1, an area in which regulation of neuroplasticity-instrumental transcription is contributed by LSD1/neuroLSD1 ratio (Wang et al., 2015; Rusconi et al., 2016). We compared two-month-old male mice carrying neuroLSD1 deletion on C57BL/6N genetic backbone (namely neuroLSD1$^{KO}$ mice), with wild type littermates. The analyses were performed in resting conditions, in which behavioral traits can already be observed (Rusconi et al., 2017). On the post synaptic side, we examined the post synaptic densities (PSDs) in terms of length, thickness, volume and abundance. It emerged that in neuroLSD1$^{KO}$ mice both length and thickness –evaluated on TEM images as previously described (Murru et al., 2017; Folci et al., 2016)– were significantly reduced (Fig. 1A). Then, plotting the size distribution of PSD length we observed that the peak of the curve is shifted leftwards, indicating an increased frequency of smaller PSDs in neuroLSD1$^{KO}$ mice (Fig. 1A). To parallel this observation about PSD size with the spine head volume, we evaluated this parameter from dendrites reconstructed from volumetric Serial Block Face - Scanning Electron Microscopy (SBF-SEM) data-sets (Fig. 1B). We found that measured dendritic spine volumes did not follow a normal distribution, as already reported (Borczyk et al., 2019). Using Mann-Whitney test to assess statistical significance, only a tendency toward decreased spine volumes in neuroLSD1$^{KO}$ mice was detected. Anyway, variation of PSD dimensions and dendritic spines volumes do not necessarily follow a superimposable trend (Borczyk et al., 2019).

For what concerns PSDs count, corresponding to excitatory synapses density, we used two different experimental techniques. Volumetric SBF-SEM data showed a tendency to reduction in neuroLSD1$^{KO}$ mice compared to wild type (1.38 ± 0.05 synapse/um$^3$ in neuroLSD1$^{KO}$ mice vs 1.47 ± 0.06 synapse/um$^3$ in wild type mice Fig. 1C). This tendency was confirmed by stereological analysis performed on TEM images (z-stack) that revealed a similar trend toward reduction in the number PSD comparing neuroLSD1$^{KO}$ mice to wild types (1.23 ± 0.06 synapse/um$^3$ in neuroLSD1$^{KO}$ mice vs 1.35 ± 0.06synapse/um$^3$ in wild type, Supplementary Fig. 1A). In parallel with ultrastructural studies, we performed optical microscopy experiments in which we stereologically analyzed CA1 dendrite images from Golgi-Cox impregnated mouse brains, observing a significant 12% decrease in spine density in neuroLSD1$^{KO}$ secondary and higher order dendrites compared to wild type (Supplementary Fig. 1B). Such a reduced spine density may arise at least in part from an optical underestimation of smaller spines, which are indeed more represented in the knock out hippocampus (EM data) and fall below the resolution power of optical microscope. However, Golgi staining analyses, together with EM data, do suggest a positive contribution of neuroLSD1 to dendritic spine biology that was further confirmed by overexpression of HA-tagged neuroLSD1 along with EGFP in primary cultured rat hippocampal neurons, leading to an increase in spine density observed with confocal microscopy (Supplementary Fig. 1C).

TEM analysis was also useful to quantitatively evaluate the presynaptic side of hippocampal excitatory synapses by measuring presynaptic areas, size and density of the synaptic vesicles pool as well as the mean vesicle diameter (Supplementary Fig. 2A) and vesicle distribution within the presynaptic bouton expressed as their distance from PSD (Cappello et al., 2012) (Supplementary Fig. 2B). All considered presynaptic parameters were not affected by neuroLSD1 deletion.

Altogether these data suggest a peculiar signature of neuroLSD1 ablation in the hippocampus in terms of dendritic spine hypotrophy and decreased PSD dimensions, forecasting inherent functional modulation of the *postsynaptic* compartment in terms of reduced E/I ratio.

### 3.2. A biochemical bridge from structure to function

We next proceeded with the biochemical evaluation of the post-synaptic compartment, employing a fractionation technique aimed at resolving the protein composition of the PSD (see methods). We chose a panel of post-synaptic components (Fig. 2A) including prominent scaffolding proteins involved in post-synaptic regulation and functionality (PSD-95, SAP97, SAP102), ionotropic glutamate, AMPA and NMDA receptors (AMPAR, NMDAR) subunits (respectively, GluA1, GluA2 and GluN1, GluN2A, GluN2B), and the immediate early protein Arc/Arg3.1.

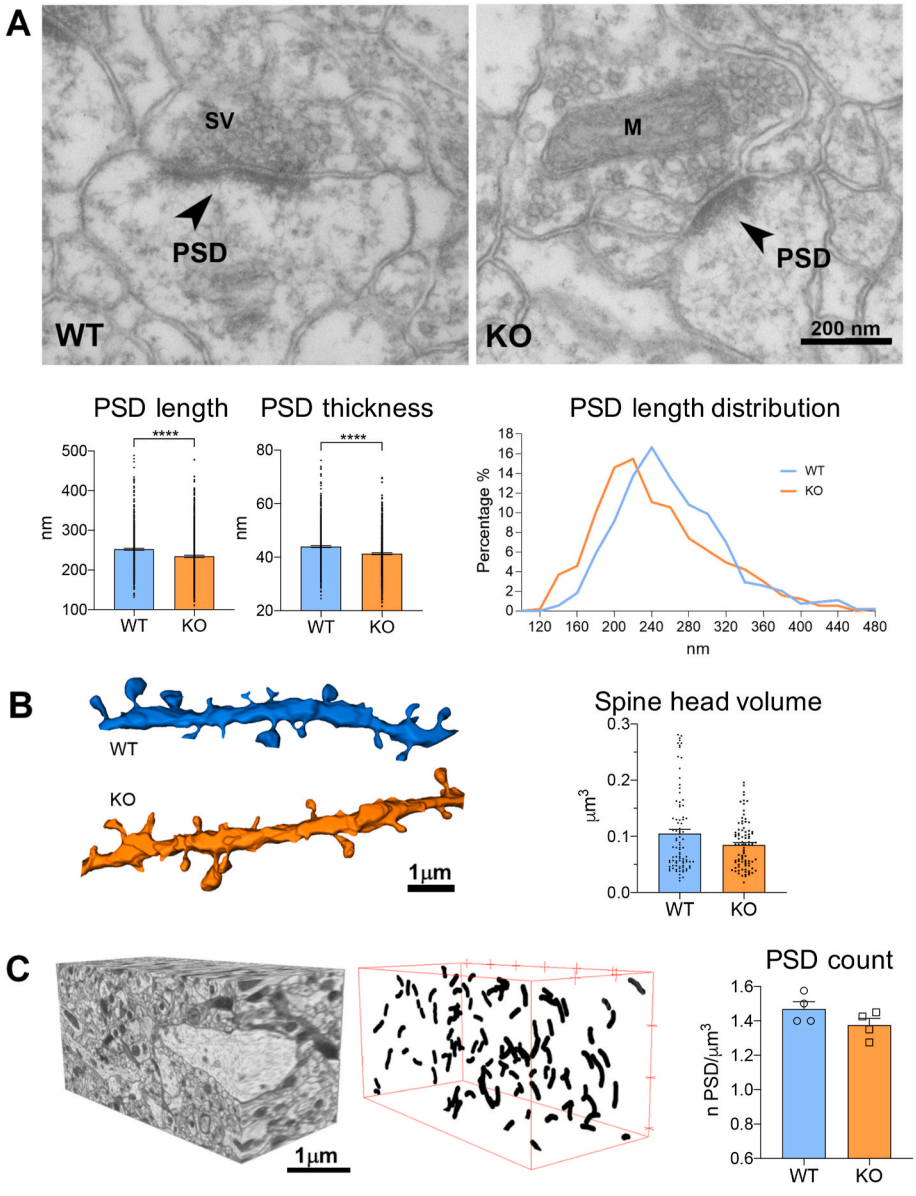


**Fig. 1.** NeuroLSD1 deletion generates an impoverished dendritic landscape at the CA1 region of the mouse hippocampus. (A) Upper Panel: Transmission Electron Microscopy (TEM) micrographs of the CA1 area of neuroLSD1$^{KO}$ mouse hippocampus compared to wild type littermates, arrows indicate post synaptic density length of representative dendritic spines. Lower Panel: mean length, thickness and PSD length distribution in WT and neuroLSD1$^{KO}$ adult mice. More than 500 synapses from three mice for each genotype were measured. (B) 3D dendritic reconstruction from SBF-SEM data-sets showing a comparison between representative dendritic segments of neuroLSD1$^{KO}$ mice CA1 area. Histogram compares spine head volumes in wild type and neuroLSD1$^{KO}$ mice calculated from Serial Block Face - Scanning Electron Microscopy (SBF-SEM) data sets. (C) Representative 3D EM image with PSDs digital reconstruction. Histogram shows PSDs count performed with SBF-SEM volumetric approach. Data are presented as means ± SEM. ****$p < 0.00001$, with Mann-Whitney test.

Interestingly, quantifying western blots performed from total hippocampal protein extracts (Fig. 2B-C-D), we observed a common trend of excitatory synaptic protein reduction, concerning all the analyzed factors in neuroLSD1$^{KO}$ mice compared to wild type littermates. However, analyzing the PSD enriched fraction, while some of these proteins were consistently reduced also at the PSD level, we found that some others increased their levels locally at the synapse. In further detail, PSD-95, an index of post-synaptic integrity and activity and similarly, the two components of AMPAR GluA1 and GluA2 were downregulated both in total hippocampus extract and at the post-synaptic density (Fig. 2B). On the contrary, all the three NMDAR subunits, GluN1, GluN2A and GluN2B, and the main scaffolding proteins of AMPAR –SAP97– and of NMDAR –SAP102– involved in glutamate receptors anchoring to the postsynaptic membrane, followed a common trend of reduction in total extracts but increased at the synapses of neuroLSD1$^{KO}$ mice compared to wild type (Fig. 2C and D). Interestingly, the immediate early protein Arc/Arg3.1, a validated direct LSD1/neuroLSD1 target which undergoes downregulation in neuroLSD1$^{KO}$ mouse cortex (Wang et al., 2015), belongs to this second group (Fig. 2D). This peculiar picture suggests a possible synaptic compensation entailing either enhanced efficiency of local translation/increased mRNA transport at the synapse or decreased protein degradation. As total protein extracts analysis showed a general decrease in synaptic components, we evaluated whether this could be due to direct LSD1 transcriptional regulation. This was the case, as we could detect differences among mRNAs encoding PSD-95, AMPAR and NMDAR subunits (Supplementary Fig. 3A). It has already been proposed that LSD1 and neuroLSD1 directly control activity-dependent transcription in neurons (Wang et al., 2015; Toffolo et al., 2014; Rusconi et al., 2016, 2017), with these data we envisage a further direct role in the modification of synaptic components. Altogether, these biochemical data indicate that diminished PSD size in neuroLSD1$^{KO}$ mice (EM data) were paralleled by decreased amounts (biochemical data) of the most abundant scaffolding protein of this compartment, namely PSD-95. Interestingly, among the analyzed post-synaptic proteins, PSD-95 is reported to increase, when overexpressed, the volume of dendritic spines (Nikonenko et al., 2008). These data suggest a direct proportion between PSD-95 amounts and dendritic spines dimensions. On the contrary, as it has been reported that Arc/Arg3.1 overexpression in primary hippocampal neurons increases the number of thin spines and filopodia (Peebles et al., 2010), Arc/Arg3.1 increase at the synapse of neuroLSD1$^{KO}$ mice well-correlates with decreased PSD size (Fig. 1A right). Interestingly, GluN1$^{KO}$ mice show considerably larger size of dendritic

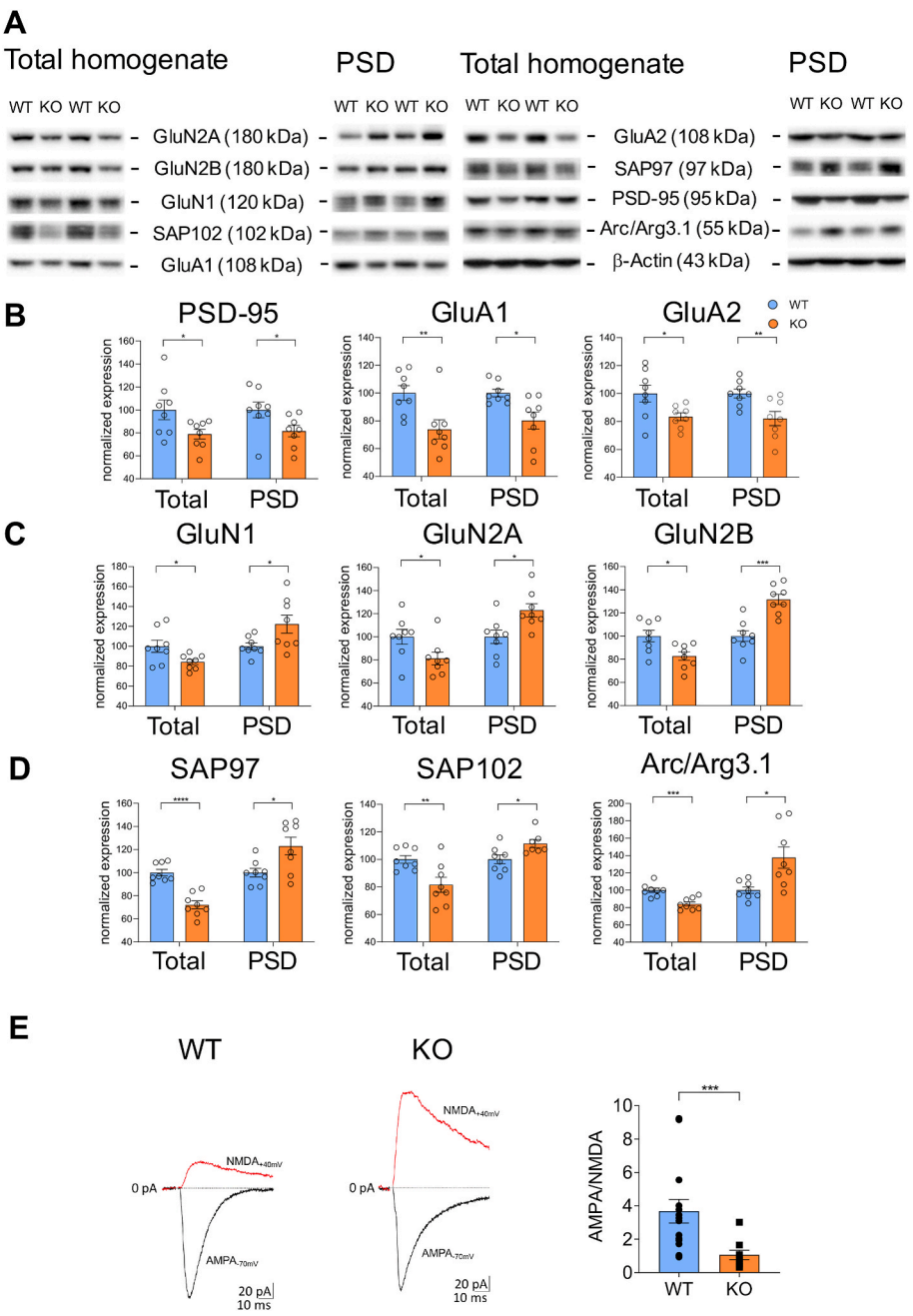


**Fig. 2.** NeuroLSD1 deletion modifies the biochemical composition of the post synaptic density (PSD). (A) Western blot analysis performed on total hippocampal extracts (Total) or PSD enriched fractions (PSD) (representative extracts from 2 wild type and 2 neuroLSD1$^{KO}$ mice are shown). (B–C-D) Densitometric profile over β-actin of indicated proteins showing a comparison of wild type and neuroLSD1$^{KO}$ littermates (normalized expression in terms of a wild type sample put to 100 in each type of protein extract). n = 8 mice for each genotype. Data are presented as means ± SEM. *p < 0.01; **p < 0.001, ***p < 0.0001, ****p < 0.00001, one-way ANOVA Tukey *post hoc* test. (E) AMPA/NMDA ratio as a function of synaptic inputs. Representative AMPA and NMDA EPSCs traces recorded at −70mV (black traces) and +40 mV (red traces) respectively. Graph shows distribution and averaged ratio for each genotype. Data are presented as means ± SEM. Mann-Whitney ***p < 0.0001. (For interpretation of the references to colour in this figure legend, the reader is referred to the Web version of this article.)

spines by the age of PND20 (Ultanir et al., 2007). This picture is compatible with the decreased PSDs sizes of neuroLSD1$^{KO}$ mice, who overexpress GluN1 at the synapses.

Notably, AMPAR and NMDAR levels diverge at the synapse of neuroLSD1$^{KO}$ mice, with a clear decrease of AMPAR subunits and increase of NMDAR components. To strengthen these data, coupling them with a functional read out, we electrophysiologically measured AMPAR/NMDAR currents in acute ex-vivo slices from adult neuroLSD1$^{KO}$ male mice compared to wild type. Consistently with biochemical data, this ratio was decreased (Fig. 2E) indicating that lack of neuroLSD1 in the mouse brain results in a resting profile of depressed excitatory synapses, and that, consequently, E/I ratio is reduced at least at the excitatory compartment.

### 3.3. *LTP impairment in neuroLSD1$^{KO}$ mice leads to memory loss*

To couple our structural and biochemical data with the search of functional neuronal endophenotypes, we measured the best characterized form of long-term plasticity, traditionally indicated as one of the foremost electrophysiological substrate of memory formation (Malenka and Bear, 2004), in neuroLSD1$^{KO}$ mice and wild type littermates. A protocol of theta burst stimulation was applied to ex-vivo acute hippocampal slices of 2-month-old male mice and synapse potentiation was measured in terms of fEPSP normalized slopes. As we could foresee from structural synaptic deficiencies, we observed impaired LTP in neuroLSD1$^{KO}$ mice, which was not completely abolished, reaching a synaptic potentiation that is reduced of about 50% (Fig. 3A). Considering that AMPAR represents a pivotal long-term potentiation (LTP) effector, its overall decrease in the context of increased NMDAR in neuroLSD1$^{KO}$ mice should be considered as a biochemical proxy to LTP impairment.

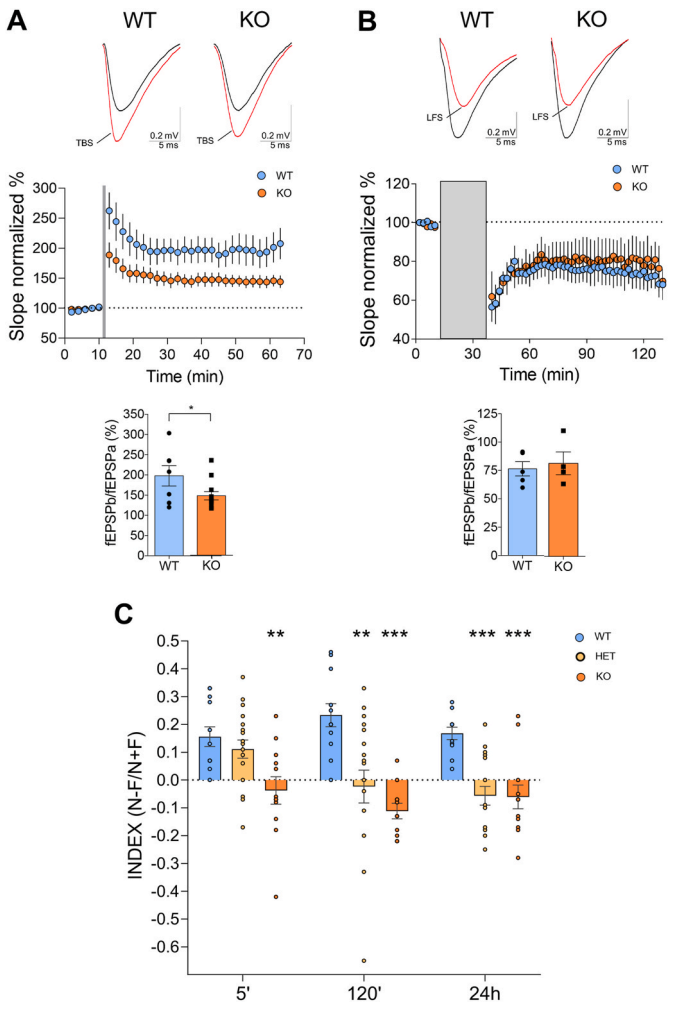


**Fig. 3.** Long term plasticity modifications coupled to memory impairment of neuroLSD1$^{KO}$ mice. (A) Theta burst stimulation (TBS)-induced Long-Term Potentiation (LTP) elicited in acute ex-vivo slices of 2-month-old male neuroLSD1$^{KO}$ mice hippocampus compared to wild type littermates (n = 7 wild type mice, n = 12 neuroLSD1$^{KO}$ mice). Upper panel, representative fEPSPs traces before (black trace) and after (red trace) TBS-LTP. Middle panel, time course of the normalized fEPSPs recording. Lower panel, ratio between WT an KO traces 35 e 45 min post-conditioning. *p < 0.05, with Student's *t*-test. (B) Low frequency stimulation (LFS)-induced Long Term Depression (LTD) elicited in acute ex-vivo slices of 2-month-old male neuroLSD1$^{KO}$ mice hippocampus neuroLSD1$^{KO}$ mice hippocampus compared to wild type littermates (n = 5 mice per genotype). Upper panel, representative fEPSPs traces before (black trace) and after (red trace) LFS-LTD. Middle panel, time course of the normalized fEPSPs recording. Lower panel, ratio between WT an KO traces 35 e 45 min post-conditioning (C) Novel Object Recognition analysis performed at 5–120 min and 24 h in 2-month-old male neuroLSD1$^{KO}$ mice (n = 12 mice per genotype). Data are presented as means ± SEM. *p < 0.01, **p < 0.001, ***p < 0.0001, two-way ANOVA coupled to Tukey *post hoc* test. (For interpretation of the references to colour in this figure legend, the reader is referred to the Web version of this article.)

However, endorsing the idea that LTP does not only represent a modification of the ionotropic glutamate receptor asset (with new AMPAR insertion in the post-synaptic membrane) but also relies on a wider neuronal rearrangement including spines structural changes (Sheng and Ertürk, 2014), we here suggest that neuroLSD1$^{KO}$ mice represent an example of integration of these molecular (biochemical PSD profile) and structural aspects (EM data). These lines of evidence prompted us to also evaluate long-term depression (LTD) in neuroLSD1$^{KO}$ mice. Indeed, the primary molecular LTD correlate is AMPAR removal from the post-synaptic membrane, but this form of plasticity is sustained over time through synapse involution entailing spine shrinkage and/or diminished volumes (Sheng and Ertürk, 2014; Li et al., 2010). LTD was measured with a protocol of low frequency stimulation (LFS). Notably, this form of long-term synaptic plasticity is fully preserved (Fig. 3B), indicating that diminished spine volumes and decreased presence of AMPAR in resting conditions does not impede, neither enhance the induction of electrophysiological synapse depression. To test the hypothesis that LTP impairment could be coupled to memory defects in neuroLSD1$^{KO}$ mice, we set a Novel Object Recognition (NOR) analysis in neuroLSD1 mutant mice. At all the three different time points analyzed, 5, 120 min and 24 h after the familial object replacement with a novel one, we observed short- and long-term memory impairment, as our animals did not spend more time exploring the novel object compared to the familial one (Fig. 3C). These data were consistent with other observations of decreased memory formation in a similar model (Wang et al., 2015). Interestingly, in our experiments, memory impairment is already present in heterozygous mice, meaning that also a physiological modulation of neuroLSD1, such as that occurring in response to a paradigm of psychosocial stress (Rusconi et al., 2016, 2017; Colombo et al., 2009) might be functional to an impairment of memory consolidation.

### 3.4. Glutamatergic nature of physiological LSD1/neuroLSD1 balance modulation

We previously reported that a single session of social defeat stress (SDS) elicits in the mouse hippocampus a transient splicing reduction of neuroLSD1 (Rusconi et al., 2016, 2017; Colombo et al., 2009). Stress triggers hippocampal glutamatergic neurons activation. This is the reason why to investigate neuronal pathways promoting LSD1/neuroLSD1 splicing response, we stimulated primary hippocampal neurons with bicuculline (BIC), a chemical paradigm aimed at excitatory neuron disinhibition via GABA receptor antagonism. Upon BIC treatment, glutamate is released exerting a synaptic stimulation that has been shown to activate both ionotropic and metabotropic glutamate receptors (Hardingham et al., 2002), along with inherent signal transduction. We stimulated primary cultured rat neurons at DIV14 for 30 min, and 8 h following BIC wash out we analyzed LSD1/neuroLSD1 splicing ratio at the mRNA level with rqfRT-PCR (Rusconi et al., 2014). We chose this time interval as we knew that in mice LSD1 splicing needs some hours to be modulated by stress (Rusconi et al., 2016, 2017). Surprisingly, BIC-treated neurons did not display differences compared to control cultures, indicating that synaptic glutamate stimulation (Hardingham et al., 2002) is not competent *per se* to challenge LSD1/neuroLSD1 ratio (Fig. 4A). We reasoned that, since environmental stress facilitates LTD induction, a long term synaptic plasticity which requires concomitant synaptic and extrasynaptic NMDAR stimulation (Papouin et al., 2012), to mimic stress effects in vitro, NMDA bath application to neuronal cultures could represent a valid alternative. We used a stimulation protocol entailing 10 min of 50 μM NMDA, featuring low or absent excitotoxic effects (Li et al., 2010). A time course experiment showed that starting from 30 min after wash out a tendency toward neuroLSD1 downregulation is evident, becoming highly significant at 2 h. At later time points neuroLSD1 transcripts almost disappear, becoming LSD1 the only splicing isoform present (Fig. 4B). Notably, total LSD1 mRNA does not significantly change (Fig. 4C), indicating a post-transcriptional splicing effect rather than neuroLSD1 mRNA degradation. We disclosed NMDAR involvement in this process as both competitive antagonist APV and the open pore NMDAR blocker MK-801 prevent LSD1/neuroLSD1 ratio modulation (Fig. 4D).

These in vitro observations gave us the chance to dissect not only the gateway of LSD1/neuroLSD1 splicing modulation, namely NMDAR stimulation, but also the importance of concomitant stimulation of synaptic and extrasynaptic NMDAR to promote such a modulation (Li et al., 2010; Papouin et al., 2012). To verify whether also in vivo LSD1/neuroLSD1 splicing modulation in response to environmental

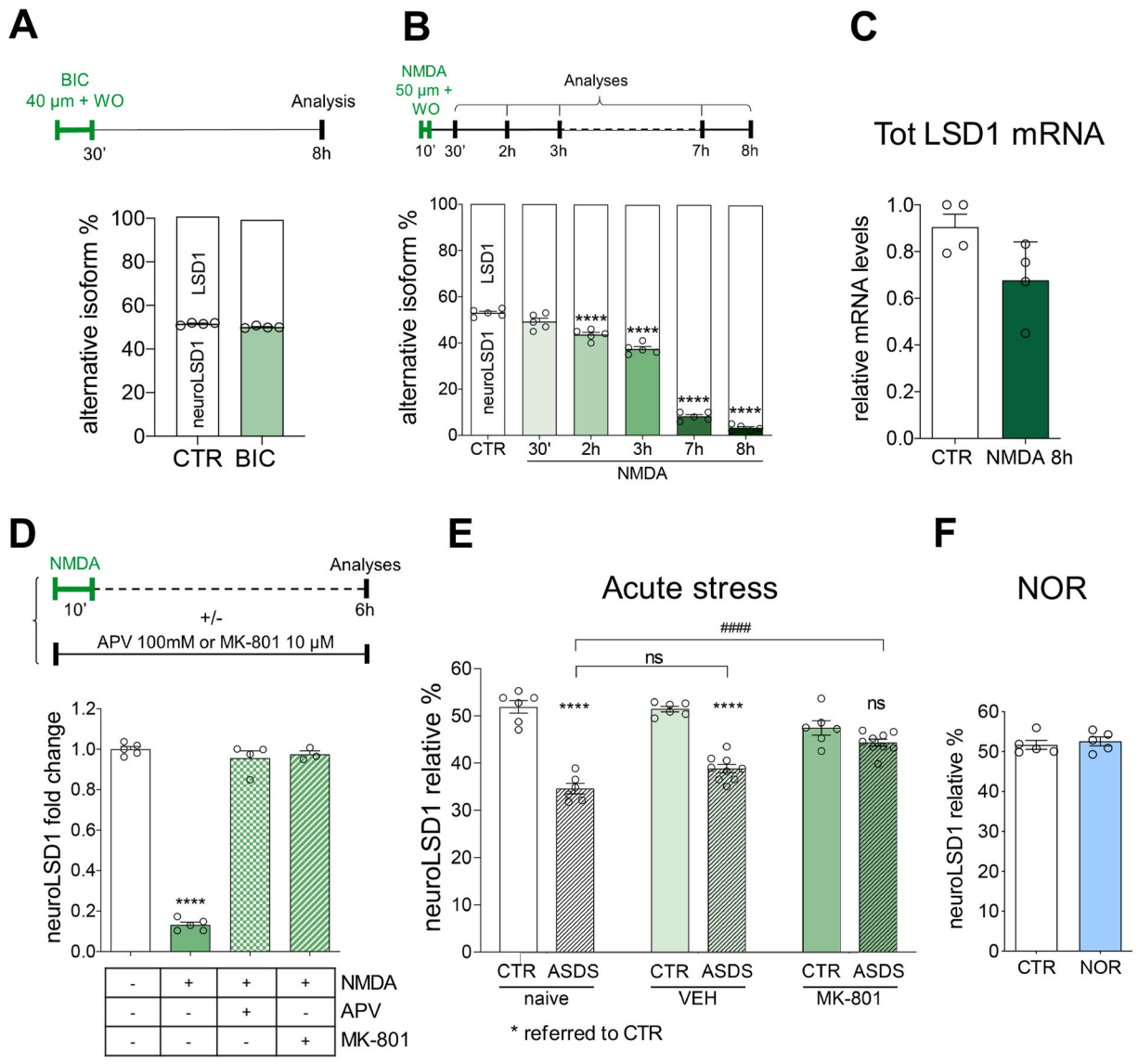


**Fig. 4.** LSD1/neuroLSD1 ratio modulation displays a specific glutamatergic drive. A) Effect of Bicuculline (BIC) treatment on DIV14 cultured hippocampal primary rat neurons (40 µM for 30 min, neurons harvested 8 h after BIC wash out, WO) over the relative ratio of the two splicing isoforms LSD1 and neuroLSD1. (B) Time course experiment showing the effect of NMDA administration to DIV14 cultured hippocampal primary rat neurons (50 µM for 10 min, neurons harvested 30 min, 2, 3,7 and 8 h after NMDA WO). *Relative to controls. (C) Total LSD1 isoforms mRNAs levels upon 50uM NMDA, neuronal cultures were incubated with NMDA for 10 min, neurons were harvested 8 h after NMDA WO. Data are presented as means ± SEM. ****$p < 0.00001$, one-way ANOVA (D) Specificity of NMDAR activation in the modulation of the relative ratio LSD1/neuroLSD1 was assessed by competitive and non-competitive NMDAR inhibitors APV and the open pore blocker MK-801. Data are presented as means ± SEM. ****$p < 0.00001$, one-way ANOVA. *Relative to controls. (E) Effects of in vivo acute social defeat stress performed in wild type 2-month-old male C57BL/6N naïve mice, vehicle-treated and MK-801 treated mice, comparing unstressed controls (CTR) with mice administered with 7 h-long stress session (ASDS, 5 min direct interaction with CD1 stressor mouse, 7 h in olfactory and visual contact with the stressor by means of a plexiglass barrier separation), over LSD1/neuroLSD1 splicing ratio in the hippocampus (n = 6 mice for each condition). *Relative to controls.elative to naïve ASDS. Data are presented as means ± SEM. ****$p < 0.00001 p < 0.00001$ two-way ANOVA coupled to Tukey *post hoc* test. (F) Effects of a learning paradigm (Familiarization phase of Novel Object Recognition, NOR) on LSD1/neuroLSD1 splicing ratio in the mouse hippocampus. Animals were sacrificed 7 h after a 20 min exposure to the same objects used for NOR in Fig. 3, (n = 5 mice per condition). Data are presented as means ± SEM.

stress is primed by glutamate stimulation of the NMDAR, we performed a single (acute) 7 h-long session of social defeat stress (ASDS) in animals systemically administered with MK-801 (0.3 mg/kg) or vehicle, 30 min before stress. As shown in Fig. 4E, MK-801 does not interfere with the basal ratio of LSD1/neuroLSD1, and vehicle-treated stressed mice behave exactly as naïve mice, significantly decreasing their hippocampal level of neuroLSD1. On the contrary, MK-801 pretreatment prevented stress-induced neuroLSD1 downregulation (Fig. 4E), in vivo supporting NMDAR involvement in the modulation of LSD1 splicing.

As we outlined that BIC-induced neuronal activation *per se* cannot trigger neuroLSD1 splicing downregulation in vitro (Fig. 4A and B, differently from NMDA bath application), we evaluated whether a different typology of environmental stimuli, such as learning in the NOR paradigm, could similarly induce LSD1/neuroLSD1 ratio modulation. As isoform ratio modulation occurs via a splicing process that requires 2–7 h (Longaretti et al., 2020), we measured neuroLSD1 relative levels in the hippocampus 7 h after object familiarization, within a window of active declarative memory consolidation. Interestingly, this paradigm did not modify LSD1/neuroLSD1 levels (Fig. 4F).

These data suggest that LSD1/neuroLSD1 ratio is modulated in the hippocampus in response to *selected* paradigms of neuronal activation including stressful situations. In this regard, we hypothesize that LSD1

splicing responses to intense glutamatergic stimuli possibly entailing synaptic and extrasynaptic NMDAR co-stimulation might hold a homeostatic nature being aimed at a transient restrainment of the glutamatergic compartment within the context of stress response.

### 3.5. An exon-skipping tool to pharmacologically decrease neuroLSD1 modifies basal synaptic glutamate transmission

Putting all the pieces of the puzzle together, we realized that i) glutamate-driven neuroLSD1 stress-induced downregulation through NMDAR ionotropic function and ii) decreased spine trophism and reduced expression of AMPAR in neuroLSD1$^{KO}$ mice, taken as a whole could represent read outs of a putative synaptic homeostatic process. Thus, we decided to test contribution of neuroLSD1 downregulation to synaptic excitability, analyzing miniature excitatory and inhibitory postsynaptic currents (mEPSCs and mIPSCs) in rat primary neurons. In particular, likewise stress (Rusconi et al., 2016), AON-mediated exon--skipping allows neuroLSD1 decrease with equal LSD1 increase. Indeed, as we told above, neuroLSD1 is an alternative LSD1 splicing isoform generated by neuron-restricted inclusion of a 12-nt long microexon, called E8a. Taking advantage of our previous study on the splicing mechanism regulating neuroLSD1 expression (Rusconi et al., 2014) that entailed splicing reporter minigene experiments, we were able to disclose that within E8a downstream intron, a palindromic *cis*-element was located, exerting a prominent negative effect against E8a inclusion (Fig. 5A). As such, deletion of this 21 nt string from the minigene (MG800-Δpal), resulted in marked upregulation of E8a inclusion in chimeric minigene-derived transcripts upon transfection in neuroblastoma cell lines (Rusconi et al., 2014). We directly used this information to design a 21 nt-long antisense oligonucleotide with the same sequence of the palindromic complementary-reverse endogenous element (AON-21-E8a), using it to promote exon E8a skipping (Fig. 5A). For thorough functional AON-21-E8a characterization see Supplementary materials and methods section and Supplementary Figs. 3C–E. We treated rat primary neurons for 36 h with the established dose of 15 μM AON-E8a-21 and performed an electrophysiological analysis aimed at measuring spontaneous synaptic transmission in terms of mEPSCs and mIPSCs. Note that used AONs were efficiently uptaken by 100% neurons, as shown by administration to the culture media of AONs covalently bound to oligothiophene fluorophore (Supplementary Fig. 3E). Remarkably, transient neuroLSD1 downregulation exerted a negative effect on both mEPSCs frequency and amplitude, in the context of

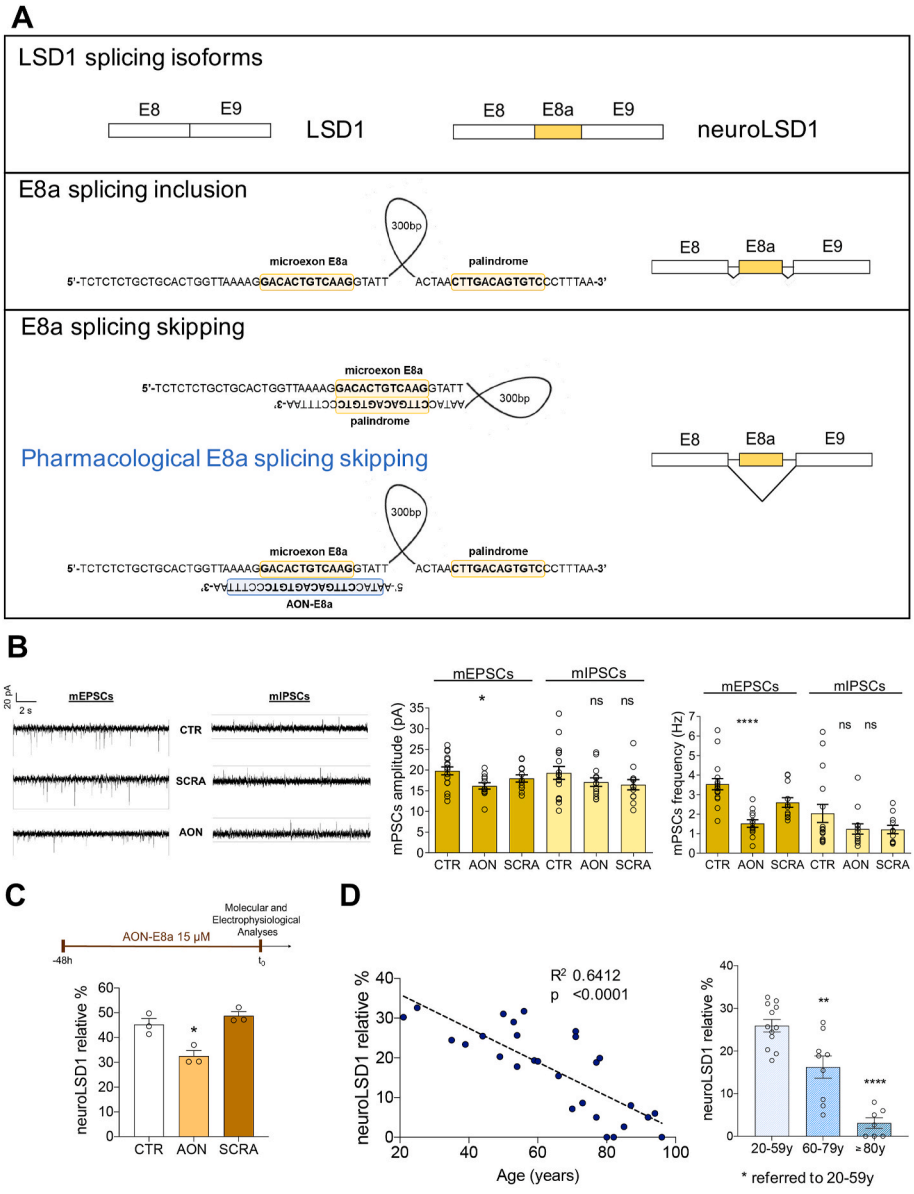


**Fig. 5.** NeuroLSD1 pharmacological inhibition in primary cultured neurons modifies EPSCs. LSD1/neuroLSD1 ratio in human brain aging. (A) Schematic representation of the palindromic E8a downstream *cis*-acting negative element, and its relative contribution to exon E8a inclusion and skipping in *LSD1* mature transcripts. Exon E8a splicing inclusion requires *cis*-acting palindromic element (palindrome) unpairing from exon E8a nucleotide sequence. Exon E8a skipping requires palindromic *or* AON-E8a-21 annealing to E8a nucleotide sequence. Note that splicing inclusion also requires trans-acting neuro-specific splicing factors NOVA1 and nSR100 (Rusconi et al., 2014), not shown. Nucleotide sequence of AON-E8a-21 is shown upside-down. (B) Exogenous AON-E8a-21-mediated LSD1/neuroLSD1 ratio modulation in cultured primary neurons impacts synaptic excitability. On the left, mEPSCs and mIPSCs currents traces. Amplitude (on the center), and frequency (on the right) of mEPSCs and mIPSCs comparing naïve, AON-E8a-21- and AON-SCRA-21-pretreated neurons. AONs were administered at a concentration of 15 μM, incubation of AON prior patch clamp electrophysiology lasted 36 h. (C) Cultures were further evaluated for AON-E8a-21-induced decrease of neuroLSD1, in comparison with AON-SCRA-21 treated cultures or untreated cultures (CTR). Data were collected from three different neuronal preparations. (D) NeuroLSD1 relative expression in the hippocampus of male and female human post-mortem specimens ranging from 20 to 94 years of age. On the left linear regression analysis describing neuroLSD1 relative expression (LSD1 + neuroLSD1 = 100%) along with aging. On the right data are aggregated per age ranges. *Refers to the youngest group. Data are presented as means ± SEM. *$p < 0.01$, ***$p < 0.0001$, ****$p < 0.00001$, one-way ANOVA coupled to Tukey *post hoc* test.

unchanged mIPSCs parameters (Fig. 5B). Every treated neuronal culture was checked for effective neuroLSD1 downregulation with rqfRT-PCR (Fig. 5C). These results suggest that in an in vitro system where neuroLSD1 downregulation is uncoupled to whatsoever glutamate signaling and transduction (i.e. an environmental stress or NMDA treatment that physiologically engage neuroLSD1 downregulation), we obtained the same effect on mEPSCs that can be obtained by eliciting homeostatic synaptic plasticity via sustained glutamate stimulation (Xu and Pozzo-Miller, 2017; Turrigiano, 2012). These data provide an in vitro perspective that neuroLSD1 downregulation upon stressful paradigms of hippocampal neuronal activation could contribute to fine tuning glutamate responses inherently decreasing synaptic excitability.

### 3.6. LSD1/neuroLSD1 modulation in the human hippocampus, an aging adaptation?

Many works described molecular and behavioral implications of LSD1 and neuroLSD1 in neurons, and in the mouse brain (Wang et al., 2015; Rusconi et al., 2014, 2016, 2017; Longaretti et al., 2020). Yet, notions of a LSD1/neuroLSD1 relevance in the human brain and possible alterations in physiological and pathological conditions have never been addressed before. To fill this gap, we decided to analyze LSD1 and neuroLSD1 expression in human cerebral tissues, sampling post-mortem female and male hippocampal specimens of different ages. We collected 10 female and 23 male hippocampal samples ranging ages 20 to 94 (Supplementary Table 1). We extracted RNAs from frozen tissues to evaluate the presence and relative ratio of the two LSD1 splicing isoforms. In detail, with rqfRT-PCR, we measured significantly decreased LSD1/neuroLSD1 ratios along with aging in both male and female hippocampi as shown by linear regression analysis and comparing individuals pooled in three age ranges, adults (20-59-year-old), seniors (60–79) and the elderly (more that 80-year-old) (Fig. 5D). These data were confirmed by qPCR analysis showing an isoform specific neuroLSD1 decrease along with aging (Supplementary Fig. 4A). Notably, when ages reach over 80 thresholds, neuroLSD1 relative expression drop to negligible levels (Fig. 5D and Supplementary Fig. 4A). Total LSD1 transcripts levels (Pan-LSD1 mRNA) measured with primers that do not discriminate the two splicing isoforms, revealed slightly decreased *LSD1* isoforms representation in the elder hippocampus (Supplementary Fig. 4B). Notably, we did not evaluate a gender effect of neuroLSD1 modulation when pooling all females and males neuroLSD1 values (Supplementary Fig. 4C). Interestingly, these data provide first evidence that LSD1/neuroLSD1 ratio undergoes age-related modulation in the human brain. Our results also suggest that within an old hippocampus, severe neuroLSD1 decrease leaves free rein to LSD1 repressive activity, opening several relevant questions about the protective or detrimental nature of such a molecular adaptation. Anyway, taking in mind impoverishment of dendritic spine morphology associated to neuroLSD1$^{KO}$ mice, stable neuroLSD1 downregulation in the human aging hippocampus (in stark contrast with transient, stress-induced neuroLSD1 decrease), well-correlates with known age-related neurostructural decline affecting both cortical and limbic structures, not to mention that neuroLSD1 decrease in the elder hippocampus likely contributes to hampering memory consolidation, a core aspect of aging.

## 4. Discussion

Within this work we propose that in response to environmental stress, along with neuronal processes devoted to associating contextual cues to the aversive paradigm (Gupta et al., 2010; Alarcón et al., 2004), a protective neurospecific mechanism opposing to memory consolidation is engaged. This mechanism is based on the splicing-mediated decrease of a neuroplasticity enhancer, namely neuroLSD1 (Rusconi et al., 2016; Longaretti et al., 2020). We here show, combining in vitro and in vivo approaches, that neuroLSD1 downregulation contributes to a negative feedback, directly elicited by glutamate via activation of the NMDAR and devoted to temporarily reduce glutamatergic synapse excitability. We already showed that a *trans*-acting splicing regulator, namely nSR100, is responsible for LSD1/neuroLSD1 splicing modulation promoting exon E8a inclusion in *LSD1* gene-derived transcripts. Interestingly, upon certain typologies of neuronal depolarization, also nSR100 levels strongly decrease (Quesnel-Vallières et al., 2016), consistently with a negative activity-dependent role on neuroLSD1 splicing generation. Activity-sensitive microexon E8a alternative splicing (allowing in neurons the co-presence of the two LSD1 isoforms, as well as their relative modulability) represents a coincidence detector of synaptic and extrasynaptic NMDAR stimulation. Indeed, only simultaneous activation of the spatially distributed NMDARs –and not the sole BIC-induced synaptic NMDAR stimulation– triggers neuroLSD1 decrease, steering neuronal plasticity toward a homeostatic reduction of synaptic excitability which, in the light of anxiolytic effects of neuroLSD1 deletion in vivo (Rusconi et al., 2016, 2017), can be interpreted as adaptive. Consistently, lack of neuroLSD1 impedes those plastic processes such as LTP, devoted to increasing neuronal excitatory responses, that again are hampered within a peculiar window of acute stress response in which formation, consolidation, and memory retrieval are temporarily occluded (Diamond et al., 2007; Zoladz et al., 2006). Interestingly, in the hippocampus these two processes –neuroLSD1 and LTP stress-induced decrease– occur within the same time window upon environmental stress exposure (Diamond et al., 2007; Rusconi et al., 2016).

The notion that hippocampal LSD1/neuroLSD1 ratio is specifically modulated by psychosocial stress but not by a *non-traumatic* learning paradigm, adds a further evidence to the elusive, but already proposed idea that environmental stress induces simultaneous stimulation of synaptic and extrasynaptic NMDARs via glutamate spill-over (Yang et al., 2005). In this regard, it is relevant to underline how an identical effect on hippocampal LSD1/neuroLSD1 ratio is triggered in response to pharmacologically-induced epilepsy (Rusconi et al., 2014). Seizures similarly to stress, entail functional correlates of hippocampal glutamate spill-over and consequent extrasynaptic NMDAR stimulation (Demarque et al., 2004; Parsons and Raymond, 2014). Intriguingly, environmental stress facilitates LTD acquisition (Wong et al., 2007), a long term plasticity requiring simultaneous NMDAR subsets activation (Papouin et al., 2012) and in vitro NMDA bath application induces chemical LTD (Sheng and Ertürk, 2014; Li et al., 2010), a process that recapitulates the morphological impoverishment of dendritic spines induced by neuroLSD1 genetic decrease. For all these evidences, we hypothesize that neuroLSD1 downregulation concurs to the well-described transient stress-induced decrease of hippocampal neuroplasticity associated to memory consolidation impairment (Diamond et al., 2007; Cadle and Zoladz, 2015).

Relevantly, we discovered that a learning paradigm (NOR) is *not* able to induce a modification of the relative ratio between LSD1 and neuroLSD1. We judge this experiment fundamental to clarify the message of our work. Checking for the effect of NOR learning on LSD1 isoforms relative ratio we ultimately had the chance to assess that *only* a stronger activation of the glutamatergic compartment, induced in the hippocampus for instance by environmental stress, pharmacological epilepsy (Rusconi et al., 2014), or mimicked in vitro by NMDA bath application, elicits *homeostatic* modifications including neuroLSD1 decrease. This experiment gives us the possibility to conclude (if interpreted in the light of the other results described in this manuscript) that neuroLSD1 downregulation takes part to an *emergency-like* program of glutamatergic restrainment. Such glutamate-buffering activity may specifically respond to the need of protecting glutamatergic circuitry from potential glutamate-related damages, meanwhile reducing traumatic memory consolidation, and is *not* engaged by a milder, learning-only, stress-devoid paradigm as the NOR. In fact, NOR paradigm quintessentially stimulates learning and memory formation and consolidation probably also because, exploiting a synaptic-restricted NMDAR stimulation, it does not modify LSD1/neuroLSD1 ratio, fully preserving the neuroplasticity enhancement function of neuroLSD1 (Rusconi et al.,

2017).

We recently provided some lines of evidence that within chronic social defeat stress, the splicing-modifying mechanism transiently regulating the relative LSD1/neuroLSD1 amount (or its activity-dependent switch), might undergo desensitization (Longaretti et al., 2020). It will be interesting to assess whether, in the light of the suggested smemorizing role of neuroLSD1 downregulation, splicing desensitization could be associated to stress susceptibility aspects, via strengthening stressful memories thereby making the negative affective stress component unforgettable. Giacomo Leopardi, a famous Italian poet of the 1800s, wrote in his poetry "Alla Luna": "Nonetheless *I enjoy the remembrance*, walking down the ages of my *sorrow*". These verses provide the poet's perspective to the idea that even if our memories can be unpleasant or traumatic, their recall and content can be softened by the fleeting nature of a resilient-like emotional information processing, to which properly balanced pro- and anti-memorizing psychobiological processes concur (Gravitz, 2019).

The relevance of our results is enhanced by human post-mortem data demonstrating the existence of LSD1 and neuroLSD1 in the human hippocampus, as well as their relative modulation during aging, further providing a new perspective to better understand the functional implications of neuroLSD1 decrease. Indeed, even if progressive physiological knock down of neuroLSD1 in the aging human hippocampus accounts for just one molecular modification among the many age-related neuronal markers, it is highly suggestive of a hypofunctional drift at the cellular, circuital, and behavioral level, possibly concurring to frailty features. On the other hand, neuroLSD1 downregulation in aging, with the complementary increase of the corepressor LSD1, could take part to a necessary trade-off aimed at preserving –at the expenses of neuroplasticity and cognitive flexibility– neuroprotection. Notably, upregulation of the transcriptional silencer REST represents, as well, a general hallmark during human brain aging. Remarkably, a causal role for REST in preserving neuronal survival, and extending lifespan, has been related to an upregulation of REST repressor function rather than to the critical level of individual REST upregulation (Zullo et al., 2019; Lu et al., 2016). All these data suggest that REST corepressors (including LSD1, CoREST and HDAC2) should play a fundamental role in enhancing REST repressive activity, downgrading synaptic genes transcription and operating a circuitry shift of E/I ratio towards reduced excitability (Zullo et al., 2019; Lu et al., 2016). This picture, as we previously published (Rusconi et al., 2014) and further show here, is phenocopied by neuroLSD1 genetic and pharmacological deletion.

## CRediT authorship contribution statement

**A. Longaretti:** Investigation, Visualization, Methodology, Data curation. **C. Forastieri:** Investigation, Visualization, Methodology, Data curation. **E. Toffolo:** Methodology. **L. Caffino:** Investigation, Methodology. **A. Locarno:** Investigation, Methodology. **I. Misevičiūtė:** Investigation. **E. Marchesi:** Methodology. **M. Battistin:** Investigation. **L. Ponzoni:** Investigation. **L. Madaschi:** Methodology, Investigation. **C. Cambria:** Investigation. **M.P. Bonasoni:** Investigation, Methodology, Data curation. **M. Sala:** Data curation. **D. Perrone:** Methodology. **F. Fumagalli:** Methodology, Data curation, Supervision. **S. Bassani:** Investigation, Supervision. **F. Antonucci:** Supervision. **R. Tonini:** Methodology, Supervision. **M. Francolini:** Methodology, Supervision. **E. Battaglioli:** Conceptualization, Data curation, Writing - original draft, Methodology, Supervision. **F. Rusconi:** Conceptualization, Data curation, Writing - original draft, Methodology, Supervision.

## Acknowledgement

We acknowledge CARIPLO Foundation grant 2016–0908 and Telethon GGP14074 to E.B., University of Milan PSR_2018 and PSR_2019 to F.R. A.L., I.M. and R.T. acknowledge the Fondazione Istituto Italiano di Tecnologia. F.F. and L.C. acknowledge grants from MIUR Progetto Eccellenza.

We acknowledge Maria Estela Andrés for stimulating discussions and critical reading of the manuscript. We acknowledge Marco Venturin for helping us with ethic committee approval and human specimens sampling. Thanks also to Marta Gritti for the generous help in LTP assessment. Thanks to Maria Italia and Valeria Casiraghi for technical support and discussions.

## Appendix A. Supplementary data

Supplementary data to this article can be found online at https://doi.org/10.1016/j.ynstr.2020.100280.

## References

Alarcón, J.M., Malleret, G., Touzani, K., Vronskaya, S., Ishii, S., Kandel, E.R., et al., 2004. Chromatin acetylation, memory, and LTP are impaired in CBP+/- mice: a model for the cognitive deficit in Rubinstein-Taybi syndrome and its amelioration. Neuron 42 (6), 947–959. https://doi.org/10.1016/j.neuron.2004.05.021.

Antonucci, F., Turola, E., Riganti, L., Caleo, M., Gabrielli, M., Perrotta, C., et al., 2012. Microvesicles released from microglia stimulate synaptic activity via enhanced sphingolipid metabolism. EMBO J. 31 (5), 1231–1240. https://doi.org/10.1038/emboj.2011.489.

Baralle, D., Baralle, M., 2005. Splicing in action: assessing disease causing sequence changes. J. Med. Genet. 42 (10), 737–748. https://doi.org/10.1136/jmg.2004.029538.

Bluett, R.J., Báldi, R., Haymer, A., Gaulden, A.D., Hartley, N.D., Parrish, W.P., et al., 2017. Endocannabinoid signalling modulates susceptibility to traumatic stress exposure. Nat. Commun. 8, 14782. https://doi.org/10.1038/ncomms14782.

Borczyk, M., Śliwińska, M.A., Caly, A., Bernas, T., Radwanska, K., 2019. Neuronal plasticity affects correlation between the size of dendritic spine and its postsynaptic density. Sci. Rep. 9 (1), 1693. https://doi.org/10.1038/s41598-018-38412-7.

Cadle, C.E., Zoladz, P.R., 2015. Stress time-dependently influences the acquisition and retrieval of unrelated information by producing a memory of its own. Front. Psychol. 6, 910. https://doi.org/10.3389/fpsyg.2015.00910.

Caffino, L., Messa, G., Fumagalli, F., 2018. A single cocaine administration alters dendritic spine morphology and impairs glutamate receptor synaptic retention in the medial prefrontal cortex of adolescent rats. Neuropharmacology 140, 209–216. https://doi.org/10.1016/j.neuropharm.2018.08.006.

Capobianco, M.L., Barbarella, G., Manetto, A., 2012. Oligothiophenes as fluorescent markers for biological applications. Molecules 17 (1), 910–933. https://doi.org/10.3390/molecules17010910.

Cappello, V., Vezzoli, E., Righi, M., Fossati, M., Mariotti, R., Crespi, A., et al., 2012. Analysis of neuromuscular junctions and effects of anabolic steroid administration in the SOD1G93A mouse model of ALS. Mol. Cell. Neurosci. 51 (1–2), 12–21. https://doi.org/10.1016/j.mcn.2012.07.003.

Carver, C.S., Scheier, M.F., 2000. Scaling back goals and recalibration of the affect system are processes in normal adaptive self-regulation: understanding 'response shift' phenomena. Soc. Sci. Med. 50 (12), 1715–1722. https://doi.org/10.1016/s0277-9536(99)00412-8.

Colombo, G., Rusconi, F., Rubino, T., Cattaneo, A., Martegani, E., Parolaro, D., et al., 2009. Transcriptomic and proteomic analyses of mouse cerebellum reveals alterations in RasGRF1 expression following in vivo chronic treatment with delta 9-tetrahydrocannabinol. J. Mol. Neurosci. 37 (2), 111–122. https://doi.org/10.1007/s12031-008-9114-2.

Colombo, G., Clerici, M., Altomare, A., Rusconi, F., Giustarini, D., Portinaro, N., et al., 2017. Thiol oxidation and di-tyrosine formation in human plasma proteins induced by inflammatory concentrations of hypochlorous acid. J Proteomics 152, 22–32. https://doi.org/10.1016/j.jprot.2016.10.008.

Demarque, M., Villeneuve, N., Manent, J.B., Becq, H., Represa, A., Ben-Ari, Y., et al., 2004. Glutamate transporters prevent the generation of seizures in the developing rat neocortex. J. Neurosci. 24 (13), 3289–3294. https://doi.org/10.1523/JNEUROSCI.5338-03.2004.

Diamond, D.M., Campbell, A.M., Park, C.R., Halonen, J., Zoladz, P.R., 2007. The temporal dynamics model of emotional memory processing: a synthesis on the neurobiological basis of stress-induced amnesia, flashbulb and traumatic memories, and the Yerkes-Dodson law. Neural Plast. 2007, 60803. https://doi.org/10.1155/2007/60803.

Duman, R.S., 2009. Neuronal damage and protection in the pathophysiology and treatment of psychiatric illness: stress and depression. Dialogues Clin. Neurosci. 11 (3), 239–255.

Folci, A., Murru, L., Vezzoli, E., Ponzoni, L., Gerosa, L., Moretto, E., et al., 2016. Myosin IXa binds AMPAR and regulates synaptic structure, LTP, and cognitive function. Front. Mol. Neurosci. 9, 1. https://doi.org/10.3389/fnmol.2016.00001.

Gravitz, L., 2019. The forgotten part of memory. Nature 571 (7766), S12–S14. https://doi.org/10.1038/d41586-019-02211-5.

Guan, J.S., Haggarty, S.J., Giacometti, E., Dannenberg, J.H., Joseph, N., Gao, J., et al., 2009. HDAC2 negatively regulates memory formation and synaptic plasticity. Nature 459 (7243), 55–60. https://doi.org/10.1038/nature07925.

Guggenhuber, S., Romo-Parra, H., Bindila, L., Leschik, J., Lomazzo, E., Remmers, F., et al., 2015. Impaired 2-AG signaling in hippocampal glutamatergic neurons:

aggravation of anxiety-like behavior and unaltered seizure susceptibility. Int. J. Neuropsychopharmacol. 19 (2) https://doi.org/10.1093/ijnp/pyv091.
Gupta, S., Kim, S.Y., Artis, S., Molfese, D.L., Schumacher, A., Sweatt, J.D., et al., 2010. Histone methylation regulates memory formation. J. Neurosci. 30 (10), 3589–3599. https://doi.org/10.1523/JNEUROSCI.3732-09.2010.
Hardingham, G.E., Fukunaga, Y., Bading, H., 2002. Extrasynaptic NMDARs oppose synaptic NMDARs by triggering CREB shut-off and cell death pathways. Nat. Neurosci. 5 (5), 405–414. https://doi.org/10.1038/nn835.
Iannotti, F.A., Di Marzo, V., Petrosino, S., 2016. Endocannabinoids and endocannabinoid-related mediators: targets, metabolism and role in neurological disorders. Prog. Lipid Res. 62, 107–128. https://doi.org/10.1016/j.plipres.2016.02.002.
Italia, M., Forastieri, C., Longaretti, A., Battaglioli, E., Rusconi, F., 2020. Rationale, Relevance and Limits of Stress-induced Psychopathology in Rodents as Models for Psychiatry Research: An Introductory Overview. Int. J. Mol. Sci. 21 (20), 7455. https://doi.org/10.3390/ijms21207455.
Kang, H.J., Voleti, B., Hajszan, T., Rajkowska, G., Stockmeier, C.A., Licznerski, P., et al., 2012. Decreased expression of synapse-related genes and loss of synapses in major depressive disorder. Nat. Med. 18 (9), 1413–1417. https://doi.org/10.1038/nm.2886.
Le François, B., Zhang, L., Mahajan, G.J., Stockmeier, C.A., Friedman, E., Albert, P.R., 2018. A novel alternative splicing mechanism that enhances human 5-HT1A receptor RNA stability is altered in major depression. J. Neurosci. 38 (38), 8200–8210. https://doi.org/10.1523/JNEUROSCI.0902-18.2018.
Leonzino, M., Ponzoni, L., Braida, D., Gigliucci, V., Busnelli, M., Ceresini, I., et al., 2019. Impaired approach to novelty and striatal alterations in the oxytocin receptor deficient mouse model of autism. Horm. Behav. 114, 104543. https://doi.org/10.1016/j.yhbeh.2019.06.007.
Li, Z., Jo, J., Jia, J.M., Lo, S.C., Whitcomb, D.J., Jiao, S., et al., 2010. Caspase-3 activation via mitochondria is required for long-term depression and AMPA receptor internalization. Cell 141 (5), 859–871. https://doi.org/10.1016/j.cell.2010.03.053.
Longaretti, A., Forastieri, C., Gabaglio, M., Rubino, T., Battaglioli, E., Rusconi, F., 2020. Termination of acute stress response by the endocannabinoid system is regulated through LSD1-mediated transcriptional repression of 2-AG hydrolases ABHD6 and MAGL. J. Neurochem., e15000 https://doi.org/10.1111/jnc.15000.
Lu, T., Aron, L., Zullo, J., Pan, Y., Kim, H., Chen, Y., et al., 2016. Addendum: REST and stress resistance in ageing and Alzheimer's disease. Nature 540 (7633), 470. https://doi.org/10.1038/nature20579.
Lutz, B., Marsicano, G., Maldonado, R., Hillard, C.J., 2015. The endocannabinoid system in guarding against fear, anxiety and stress. Nat. Rev. Neurosci. 16 (12), 705–718. https://doi.org/10.1038/nrn4036.
Malenka, R.C., Bear, M.F., 2004. LTP and LTD: an embarrassment of riches. Neuron 44 (1), 5–21. https://doi.org/10.1016/j.neuron.2004.09.012.
Morena, M., Patel, S., Bains, J.S., Hill, M.N., 2016. Neurobiological interactions between stress and the endocannabinoid system. Neuropsychopharmacology 41 (1), 80–102. https://doi.org/10.1038/npp.2015.166.
Murru, L., Vezzoli, E., Longatti, A., Ponzoni, L., Falqui, A., Folci, A., et al., 2017. Pharmacological modulation of AMPAR rescues intellectual disability-like phenotype in Tm4sf2-/y mice. Cerebr. Cortex 27 (11), 5369–5384. https://doi.org/10.1093/cercor/bhx221.
Nikonenko, I., Boda, B., Steen, S., Knott, G., Welker, E., Muller, D., 2008. PSD-95 promotes synaptogenesis and multiinnervated spine formation through nitric oxide signaling. J. Cell Biol. 183 (6), 1115–1127. https://doi.org/10.1083/jcb.200805132.
Papouin, T., Ladépêche, L., Ruel, J., Sacchi, S., Labasque, M., Hanini, M., et al., 2012. Synaptic and extrasynaptic NMDA receptors are gated by different endogenous coagonists. Cell 150 (3), 633–646. https://doi.org/10.1016/j.cell.2012.06.029.
Parsons, M.P., Raymond, L.A., 2014. Extrasynaptic NMDA receptor involvement in central nervous system disorders. Neuron 82 (2), 279–293. https://doi.org/10.1016/j.neuron.2014.03.030.
Patel, S., Shonesy, B.C., Bluett, R.J., Winder, D.G., Colbran, R.J., 2016. The anxiolytic actions of 2-arachidonoylglycerol: converging evidence from two recent genetic endocannabinoid deficiency models. Biol. Psychiatr. 79 (10), e78–e79. https://doi.org/10.1016/j.biopsych.2015.04.028.
Peebles, C.L., Yoo, J., Thwin, M.T., Palop, J.J., Noebels, J.L., Finkbeiner, S., 2010. Arc regulates spine morphology and maintains network stability in vivo. Proc. Natl. Acad. Sci. U. S. A. 107 (42), 18173–18178. https://doi.org/10.1073/pnas.1006546107.
Pfaffl, M.W., Tichopad, A., Prgomet, C., Neuvians, T.P., 2004. Determination of stable housekeeping genes, differentially regulated target genes and sample integrity: BestKeeper–Excel-based tool using pair-wise correlations. Biotechnol. Lett. 26 (6), 509–515. https://doi.org/10.1023/b:bile.0000019559.84305.47.
Pitsikas, N., Rigamonti, A.E., Cella, S.G., Locatelli, V., Sala, M., Muller, E.E., 2001. Effects of molsidomine on scopolamine-induced amnesia and hypermotility in the rat. Eur. J. Pharmacol. 426 (3), 193–200. https://doi.org/10.1016/s0014-2999(01)01164-5.
Popoli, M., Yan, Z., McEwen, B.S., Sanacora, G., 2012. The stressed synapse: the impact of stress and glucocorticoids on glutamate transmission. Nat. Rev. Neurosci. 13 (1), 22–37. https://doi.org/10.1038/nrn3138.
Prini, P., Rusconi, F., Zamberletti, E., Gabaglio, M., Penna, F., Fasano, M., et al., 2018. Adolescent THC exposure in female rats leads to cognitive deficits through a mechanism involving chromatin modifications in the prefrontal cortex. J. Psychiatry Neurosci. 43 (2), 87–101.
Quesnel-Vallières, M., Dargaei, Z., Irimia, M., Gonatopoulos-Pournatzis, T., Ip, J.Y., Wu, M., et al., 2016. Misregulation of an activity-dependent splicing network as a common mechanism underlying autism spectrum disorders. Mol. Cell. 64 (6), 1023–1034. https://doi.org/10.1016/j.molcel.2016.11.033.
Rimessi, P., Sabatelli, P., Fabris, M., Braghetta, P., Bassi, E., Spitali, P., et al., 2009. Cationic PMMA nanoparticles bind and deliver antisense oligoribonucleotides allowing restoration of dystrophin expression in the mdx mouse. Mol. Ther. 17 (5), 820–827. https://doi.org/10.1038/mt.2009.8.
Rodríguez-Muñoz, M., Sánchez-Blázquez, P., Merlos, M., Garzón-Niño, J., 2016. Endocannabinoid control of glutamate NMDA receptors: the therapeutic potential and consequences of dysfunction. Oncotarget 7 (34), 55840–55862. https://doi.org/10.18632/oncotarget.10095.
Romorini, S., Piccoli, G., Jiang, M., Grossano, P., Tonna, N., Passafaro, M., et al., 2004. A functional role of postsynaptic density-95-guanylate kinase-associated protein complex in regulating Shank assembly and stability to synapses. J. Neurosci. 24 (42), 9391–9404. https://doi.org/10.1523/JNEUROSCI.3314-04.2004.
Rusconi Ph.D, F., et al., Rubino Tiziana, 2020. Endocannabinoid-Epigenetic Crosstalk: A Bridge Towards Stress Coping. Int. J. Mol. Sci. 21 (17), 6252. https://doi.org/10.3390/IJMS21176252.
Rusconi, F., Battaglioli, E., 2018. Acute stress-induced epigenetic modulations and their potential protective role toward depression. Front. Mol. Neurosci. 11, 184. https://doi.org/10.3389/fnmol.2018.00184.
Rusconi, F., Paganini, L., Braida, D., Ponzoni, L., Toffolo, E., Maroli, A., et al., 2014. LSD1 neurospecific alternative splicing controls neuronal excitability in mouse models of epilepsy. Cerebr. Cortex. https://doi.org/10.1093/cercor/bhu070.
Rusconi, F., Grillo, B., Ponzoni, L., Bassani, S., Toffolo, E., Paganini, L., et al., 2016. LSD1 modulates stress-evoked transcription of immediate early genes and emotional behavior. Proc. Natl. Acad. Sci. U. S. A. 113 (13), 3651–3656. https://doi.org/10.1073/pnas.1511974113.
Rusconi, F., Grillo, B., Toffolo, E., Mattevi, A., Battaglioli, E., 2017. NeuroLSD1: splicing-generated epigenetic enhancer of neuroplasticity. Trends Neurosci. 40 (1), 28–38. https://doi.org/10.1016/j.tins.2016.11.002.
Rusconi, F., Battaglioli, E., Venturin, M., 2020. Psychiatric disorders and lncRNAs: a synaptic match. Int. J. Mol. Sci. 21 (9) https://doi.org/10.3390/ijms21093030.
Sanacora, G., Treccani, G., Popoli, M., 2012. Towards a glutamate hypothesis of depression: an emerging frontier of neuropsychopharmacology for mood disorders. Neuropharmacology 62 (1), 63–77. https://doi.org/10.1016/j.neuropharm.2011.07.036.
Saunderson, E.A., Spiers, H., Mifsud, K.R., Gutierrez-Mecinas, M., Trollope, A.F., Shaikh, A., et al., 2016. Stress-induced gene expression and behavior are controlled by DNA methylation and methyl donor availability in the dentate gyrus. Proc. Natl. Acad. Sci. U. S. A. 113 (17), 4830–4835. https://doi.org/10.1073/pnas.1524857113.
Sheng, M., Ertürk, A., 2014. Long-term depression: a cell biological view. Philos. Trans. R. Soc. Lond. B Biol. Sci. 369 (1633), 20130138. https://doi.org/10.1098/rstb.2013.0138.
Shonesy, B.C., Bluett, R.J., Ramikie, T.S., Báldi, R., Hermanson, D.J., Kingsley, P.J., et al., 2014. Genetic disruption of 2-arachidonoylglycerol synthesis reveals a key role for endocannabinoid signaling in anxiety modulation. Cell Rep. 9 (5), 1644–1653. https://doi.org/10.1016/j.celrep.2014.11.001.
Toffolo, E., Rusconi, F., Paganini, L., Tortorici, M., Pilotto, S., Heise, C., et al., 2014. Phosphorylation of neuronal Lysine-Specific Demethylase 1LSD1/KDM1A impairs transcriptional repression by regulating interaction with CoREST and histone deacetylases HDAC1/2. J. Neurochem. 128 (5), 603–616. https://doi.org/10.1111/jnc.12457.
Turrigiano, G., 2012. Homeostatic synaptic plasticity: local and global mechanisms for stabilizing neuronal function. Cold Spring Harb Perspect Biol 4 (1), a005736. https://doi.org/10.1101/cshperspect.a005736.
Ultanir, S.K., Kim, J.E., Hall, B.J., Deerinck, T., Ellisman, M., Ghosh, A., 2007. Regulation of spine morphology and spine density by NMDA receptor signaling in vivo. Proc. Natl. Acad. Sci. U. S. A. 104 (49), 19553–19558. https://doi.org/10.1073/pnas.0704031104.
Vezzoli, E., Calì, C., De Roo, M., Ponzoni, L., Sogne, E., Gagnon, N., et al., 2020. Ultrastructural evidence for a role of astrocytes and glycogen-derived lactate in learning-dependent synaptic stabilization. Cerebr. Cortex 30 (4), 2114–2127. https://doi.org/10.1093/cercor/bhz226.
Wang, J., Telese, F., Tan, Y., Li, W., Jin, C., He, X., et al., 2015. LSD1n is an H4K20 demethylase regulating memory formation via transcriptional elongation control. Nat. Neurosci. 18 (9), 1256–1264. https://doi.org/10.1038/nn.4069.
Wong, T.P., Howland, J.G., Robillard, J.M., Ge, Y., Yu, W., Titterness, A.K., et al., 2007. Hippocampal long-term depression mediates acute stress-induced spatial memory retrieval impairment. Proc. Natl. Acad. Sci. U. S. A. 104 (27), 11471–11476. https://doi.org/10.1073/pnas.0702308104.
Xu, X., Pozzo-Miller, L., 2017. EEA1 restores homeostatic synaptic plasticity in hippocampal neurons from Rett syndrome mice. J. Physiol. 595 (16), 5699–5712. https://doi.org/10.1113/JP274450.

Yang, C.H., Huang, C.C., Hsu, K.S., 2005. Behavioral stress enhances hippocampal CA1 long-term depression through the blockade of the glutamate uptake. J. Neurosci. 25 (17), 4288–4293. https://doi.org/10.1523/JNEUROSCI.0406-05.2005.

Zibetti, C., Adamo, A., Binda, C., Forneris, F., Toffolo, E., Verpelli, C., et al., 2010. Alternative splicing of the histone demethylase LSD1/KDM1 contributes to the modulation of neurite morphogenesis in the mammalian nervous system. J. Neurosci. 30 (7), 2521–2532. https://doi.org/10.1523/JNEUROSCI.5500-09.2010.

Zoladz, P.R., Campbell, A.M., Park, C.R., Schaefer, D., Danysz, W., Diamond, D.M., 2006. Enhancement of long-term spatial memory in adult rats by the noncompetitive NMDA receptor antagonists, memantine and neramexane. Pharmacol. Biochem. Behav. 85 (2), 298–306. https://doi.org/10.1016/j.pbb.2006.08.011.

Zullo, J.M., Drake, D., Aron, L., O'Hern, P., Dhamne, S.C., Davidsohn, N., et al., 2019. Regulation of lifespan by neural excitation and REST. Nature 574 (7778), 359–364. https://doi.org/10.1038/s41586-019-1647-8.